Although it is true that the world history of modern crystèllography is now rather old, its continuing achievements have provided indispensable knowledge and tools for the future progress of science in general. On the other hand, it is also true that the frontiers of crystallography and related fields are ever growing into innumerable branches so rapidly and so manifoldly that it cannot be denied that one is likely to be lost in orientation in the midst of such a wealth of scientific activities.

References

FURUSAKI, A. TOMIIE, Y. & NITTA, I. (1970). *Bull. Chem. Soc. Japan*, **43**, 3332–3341.

KIRIYAMA, R., YABUMOTO, S. & NITTA, I. (1954). *Bull. Chem. Soc. Japan*, **27**, 115–119.

NISHIKAWA, S. & ONO, S. (1913). *Proc. Math. Phys. Soc. Tokyo*, **7**, 131–298.

NITTA, I. (1940). *Sci. Papers Inst. Phys. Chem. Research, Tokyo*, **37**, 114–130.

NITTA, I., SEKI, S. & MOMOTANI, M. (1950). *Proc. Japan. Acad.* **26**, No. 9, 25–29.

NITTA, I., SEKI, S., MOMOTANI, M., SUZUKI, K. & NAKAGAWA, S. (1950). *Proc. Japan. Acad.* **26**, No. 10, 11–1*c*.8.

OGAWA, S. & WATANABE, D. (1954). *J. Phys. Soc. Japan*, **9**, 475–488.

SAITO, Y., NAKATSU, K., SHIRO, M. & KUROYA, H. (1954). *Acta Cryst.* **7**, 636.

YUKITOSHI, T., SUGA, H., SEKI, S. & ITOH, J. (1957). *J. Phys. Soc. Japan*, **12**, 506–515.

Acta Cryst. (1973). A**29**, 322

Structure Determination of a $MoO_2Cl_2.H_2O$ Polytype by Interpretation of Non-Space-Group Extinctions*

BY H. SCHULZ

Institut für Kristallographie und Petrographie, ETH, CH-8006 Zürich, Sonneggstrasse 5, Switzerland

AND F. A. SCHRÖDER

Lehrstuhl für Anorganische Chemie der Universität, D-7800 Freiburg i. Br., Albertstrasse 21, Germany (BRD)

(*Received* 23 *April* 1972; *accepted* 17 *November* 1972)

Based on the magnitude of intensities obtained by X-ray diffraction, the reflexions of $MoO_2Cl_2.H_2O$ can be divided into so-called main reflexions (strong intensities) and so-called superstructure reflexions (weak intensities). A comparison of the structure determined with the main reflexions only (designated as structure *A*) and of the structure determined with the superstructure reflexions only (designated as structure *B*) shows that structure *A* is not the superposition or average structure of structure *B*, but that structures *A* and *B* are polytypes. This means that the basic structure element, the coordination polyhedron of the Mo atoms, being an irregular octahedron, is very similar in both structures. The octahedra are however combined with each other in different ways in the two structures.

1. Structure *A*

Structure *A* was determined by Atovmyan & Aliev (1971) and Schröder & Nørlund Christensen (1972). It crystallizes in space group $Pmn2_1$. The cell dimensions are $a=9{\cdot}23$, $b=3{\cdot}89$, $c=91$ Å. The projection of the structure on (100) is shown in Fig. 1(*a*). The main feature of structure *A* is the coordination polyhedron around Mo in form of an irregular octahedron. The Mo atom is displaced from the centre into a tetrahedral environment, which must be considered as the essential bonding polyhedron. The four atoms forming the corners of the tetrahedron are mainly bonded to the corresponding Mo atom. In Fig. 2 the sequence of the polyhedra in structure *A* for two unit cells is shown. Each unit cell contains two octahedra. Each octahedron is part of a chain running parallel to the *b* axis. The octahedra have two common edges. The two chains can be considered as antiparallel.

During the collection of the data three crystals were investigated, all of which showed besides the reflexions corresponding to structure *A*, additional superstructure reflexions which are considered separately in this paper.

2. Explanation of the terms, position of gravity, ideal position and real position

In the following, some general considerations are outlined: Fig. 3 shows in (*a*) an arrangement of two Mo atoms in cell *A*. In (*b*) four cells *A* are put together in

* Part VIII of Contributions to the Chemistry of Molybdenum and Tungsten. For part VII see: *Z. anorg. algem. Chem.* (1972), **392**, 107.

atoms in cell *A*. In (*b*) four cells *A* are put together in order to form one cell, called *B*. In this manner the arrangement of the Mo atoms in cell *A* is formally

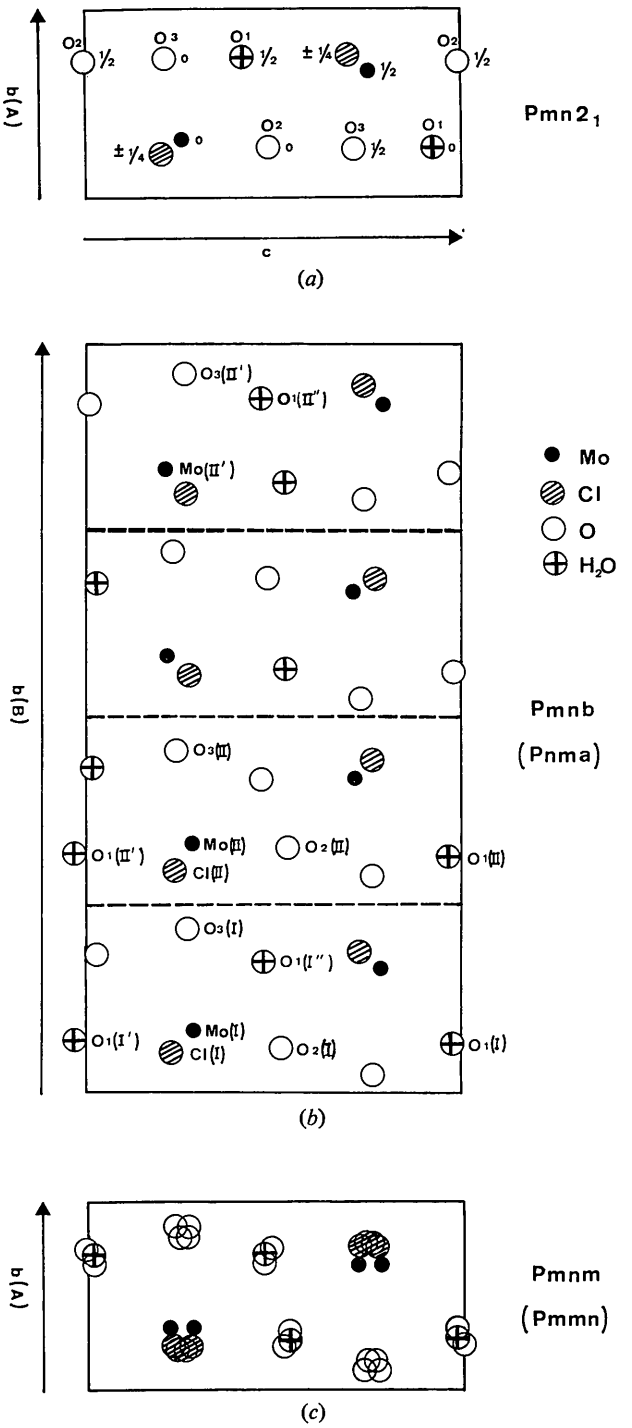

Fig. 1. (*a*) Projection of structure *A* on (100). (*b*) Projection of structure *B* on (100). (*c*) Projection of the average structure of structure *B* on (100).

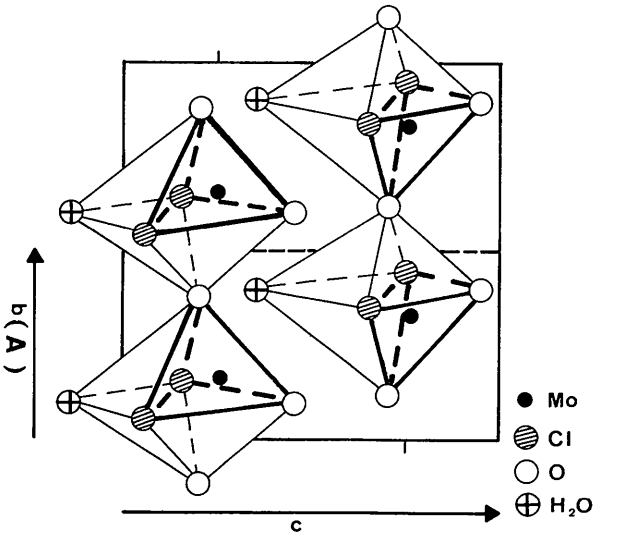

Fig. 2. Arrangement of the coordination polyhedra of two unit cells of structure *A*.

transformed into a cell *B*. The Mo arrangement in (*c*) is generated by displacing the Mo atoms from the positions shown in (*b*) according to the arrows.

The Mo positions of (*a*), (*b*), (*c*) are designated as positions of gravity, ideal positions and real positions respectively. The term position of gravity can be understood in the following way: If cell *B* in (*c*) is subdivided into four cells *A* and if these four cells are superimposed, the atomic arrangement of (*d*) is generated. It represents the so-called superposition or average structure of (*c*). This atomic arrangement can be described as two sets of split atoms. The corresponding positions of gravity of these split atoms coincide with the positions of the Mo atoms in (*a*). Therefore these positions are designated as positions of gravity.

In diffraction experiments the atomic arrangement of (*c*) would produce so-called main and superstructure reflexions. The mean of the diffracted intensities of the main reflexions is considerably stronger than the corresponding value of the superstructure reflexions. For the atomic arrangement of (*c*) main reflexions and superstructure reflexions are characterized by *hkl* indices $k=4n$, and $k\neq 4n$ respectively. The arrangement of (*b*) does not produce superstructure reflexions, but only main reflexions.

The refinement of the structure of cell *B* was carried out with the observed and pseudo-extinct superstructure reflexions only [collected, together with the main reflexions, at the University of Aarhus (*cf.* Schröder & Nørlund Christensen, 1972)], and not with a mixed data set of main and superstructure reflexions. This is a necessary consequence of a structure model existing for the main reflexions but not for the superstructure reflexions. Superstructure models must therefore be tested by comparing the *F* values of cal-

culated and observed superstructure reflexions only. As these reflexions are generally characterized by weak intensities compared with the main reflexions, incorrect models may be tolerated because a poor agreement between F values of observed and calculated superstructure reflexions is masked by a good agreement between observed and calculated F values of the main reflexions. This happens if the positions of gravity calculated from the incorrect superstructure model agree with the atomic positions of the model derived from the main reflexions.

3. Non-space-group extinctions

The cell constants derived from the main reflexions (cell A) (Schröder & Nørlund Christensen, 1972) and from the superstructure reflexions (cell B) show the following relations:

$$a(B)=a\,(A)$$
$$b(B)=4b\,(A)$$
$$c(B)=c\,(A).$$

Using the lattice constants of cell B, main and superstructure reflexions have the following hkl values:

main reflexions: hkl with $k=4n$
superstructure reflexions: hkl with $k\neq 4n$.

The following non-space-group extinctions were observed:

1. $F(hkl)$ not present, if $k=4n+2$
2. $F(hk0)$ not present, if $k\neq 4n$.

A schematic presentation of the diffraction pattern is shown in Fig. 4.

The first non-space-group extinction is designated as a pseudo-extinction rule according to Niggli (1959). From its interpretation follows: If in cell B an atom occupies a position (x,y,z), another atom must occupy the position $(x,y+\frac{1}{4},z)$ or $(x,y-\frac{1}{4},z)$.

The second extinction was interpreted in the following way: the atoms in structure B deviate from ideal positions. It also shows, that the atoms are shifted away from these ideal positions parallel to the c axis only, by $\pm\Delta z$.*

So in Fig. 3 cell B contains two times four Mo atoms occupying ideal positions as shown in (b). In (c) the interpretations of the two non-space-group extinctions are combined. This means that the atoms are shifted from their ideal positions of (b) in the manner shown. This atomic arrangement produces a diffraction pattern as given by the experiment. In other words, the atom occupying the ideal position of Mo(1) in (b) is shifted from this position by $+\Delta z$ in (c). As a consequence of the first extinction the atom Mo(2) must be shifted from the ideal position by $+\Delta z$ too. This arrangement of two atoms already fulfils the interpretation of both non-space-group extinctions. In order to get the position of gravity of (a), the remaining atoms Mo(3) and Mo(4) must be shifted from the ideal positions by $-\Delta z$. The same arguments hold for the atoms Mo(5) to Mo(8).

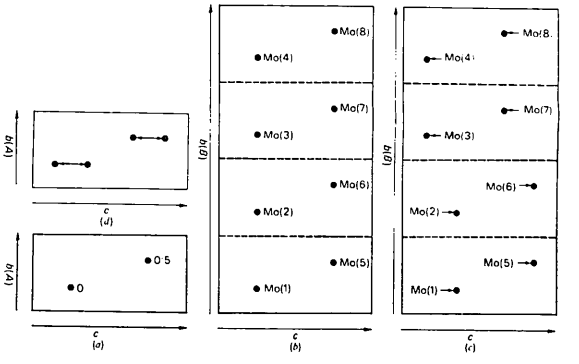

Fig. 3. Derivation of superstructure models for the Mo atoms. (a) Mo positions in cell A; (b) Corresponding ideal Mo positions in cell B; (c) Superstructure model of the Mo atoms in agreement with the non space-group extinctions; (d) Superposition structure derived from (c).

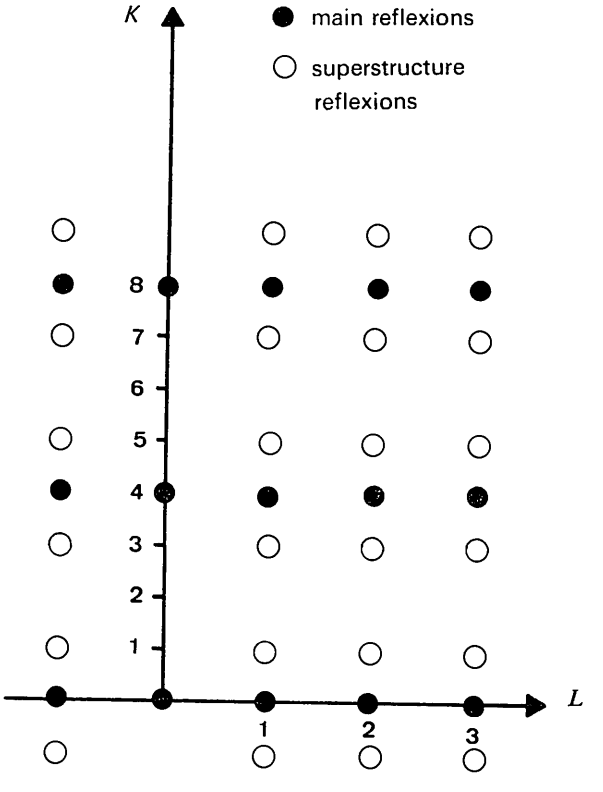

Fig. 4. Schematic presentation of the diffraction pattern, according to the photograph in Fig. 2 of Schröder & Nørlund Christensen (1972).

* This was already strongly indicated by the remarkable elongation of the thermal vibrational ellipsoids parallel to the c axis of the atoms in structure A.

Thus, it has to be concluded that, if an atom in cell B occupies the position

$$x,y,z+\Delta z,$$

there must be three other atoms of the same sort occupying the positions

$$x, y+\tfrac{1}{4}, z+\Delta z$$
$$x, y+\tfrac{2}{4}, z-\Delta z$$
$$x, y+\tfrac{3}{4}, z-\Delta z\,.$$

This means that, by determining the position of one atom in cell B, the positions of three other atoms of the same sort are determined.

4. Patterson synthesis using superstructure reflexions only

A Patterson synthesis using superstructure reflexions only was calculated in order to determine which atoms mainly contribute to the intensities of the superstructure reflexions. The main feature of this Patterson synthesis is a strong maximum in $\pm(uvw)=\pm(0{\cdot}5, 0{\cdot}16, 0{\cdot}5)$. This maximum is accompanied by two 'satellite' minima, with a depth half as strong as the maximum. These minima have the same u and v coordinates as the maximum. Their w coordinates are $w=0{\cdot}5\pm0{\cdot}1$. This is shown in Fig. 5. The strong maximum is caused by the Mo atoms. This can be proved in the following way: in structure A the Mo atoms occupy the equivalent positions 2(a) of space group $Pmn2_1$ with the coordinates

$$0,y,z \text{ and } \tfrac{1}{2}, -y, \tfrac{1}{2}+z\,.$$

The ideal positions in cell B as shown for the Mo atoms in Fig. 3(b) are listed in Table 1. The Patterson vectors between the atoms (1) and (5), (2) and (6) and so on have the coordinates:

$$\pm(uvw)=\pm(0{\cdot}5, 2y/4, 0{\cdot}5)\,.$$

Using the y coordinate of Mo in structure A ($y=0{\cdot}32$), we get the corresponding Mo–Mo vector:

$$(uvw)=(0{\cdot}5, 0{\cdot}16, 0{\cdot}5)\,.$$

These values are just the coordinates of the strongest Patterson peak. Similar calculations with the remaining atomic positions of structure A show that no further vectors exist which can be related to this strongest peak of the Patterson synthesis. Therefore for the first step of a structure determination based on the superstructure reflexions, the Mo atoms must be considered. The arrangement of a maximum accompanied by two satellite minima is a typical feature for superstructures caused by displacements. The vectors from the maxi-

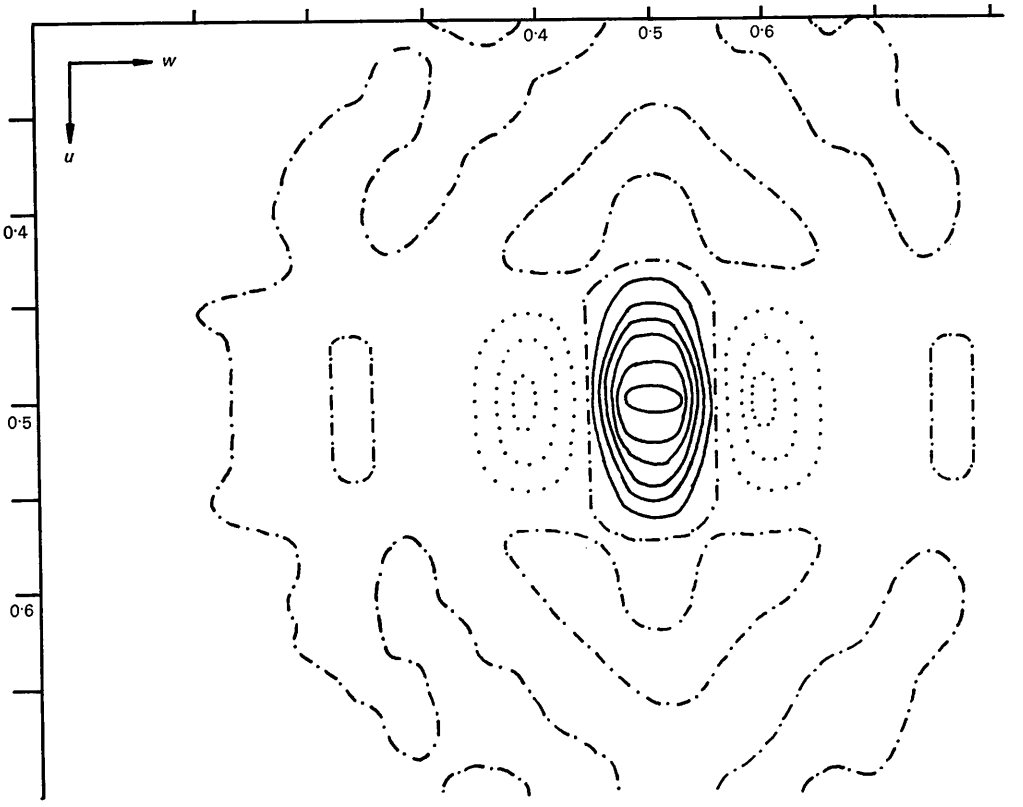

Fig. 5. Patterson section at $v=0{\cdot}16$. Full lines mark positive values, dotted lines mark negative values.

mum to the minima give the directions of displacements. In our case they are parallel to **c**. They confirm the interpretation of the second non-space-group extinction. Thus $|\Delta z|$ of the Mo atoms can be estimated from the separation of the satellite minima from their maximum. It holds that

$$|\Delta z| = |\Delta w/2| = 0{\cdot}1/2 = 0{\cdot}05 .$$

Table 1. *Ideal positions for the* Mo *atoms in cell B*

(1)	0	$y/4$	z	(5)	$\frac{1}{2}$	$-y/4$	$z+\frac{1}{2}$
(2)	0	$y/4+\frac{1}{4}$	z	(6)	$\frac{1}{2}$	$-y/4+\frac{1}{4}$	$z+\frac{1}{2}$
(3)	0	$y/4+\frac{2}{4}$	z	(7)	$\frac{1}{2}$	$-y/4+\frac{2}{4}$	$z+\frac{1}{2}$
(4)	0	$y/4+\frac{3}{4}$	z	(8)	$\frac{1}{2}$	$-y/4+\frac{3}{4}$	$z+\frac{1}{2}$

5. Superstructure models for the Mo atoms

With the foregoing results we are able to construct superstructure models for the Mo atoms. It can be shown that there are only 4 possible models. They can be derived from the atomic arrangement of Mo atoms in structure *A*. The coordinates of the ideal positions can be calculated by means of Table 1 using the Mo coordinates of structure *A* (0, 0·32, 0·25). The groups of Mo(1) to Mo(4) and Mo(5) to Mo(8) atoms as given in Fig. 3(*b*), each have the same x and z coordinates. These atoms must be shifted in position according to Fig. 3(*c*). This means one Mo atom of each group can be selected arbitrarily as 'starting atom' to be displaced by $+\Delta z$. By this operation the positions of all atoms of one group are determined as shown in §3. We used Mo(1) and Mo(5), the Mo atoms with the lowest y values, as starting atoms.

In order to derive the true superstructure out of all possible combinations the arrangement of Mo(1) to Mo(4) was kept unaltered. Each of the atoms Mo(5) to Mo(8) was used as 'starting atom', which is displaced by $+\Delta z$ and which determines the positions of the remaining three as shown in §2. These four models are listed in Table 2. They were used for structure-factor calculations with 322 diffractometer-measured superstructure reflexions with $F_o \neq 0$. The corresponding *R* values are also listed in Table 2. The best *R* value was given by model 4. This was used for calculating a Fourier synthesis using again superstructure reflexions only.*

* The same scattering-factor values were used as in the paper of Schröder & Nørlund Christensen (1972). The refinement was done with the full-matrix least-squares program of Busing, Martin & Levy (1962).

6. Symmetry considerations of structure *B*

The Fourier synthesis described in §5 showed additional strong maxima besides the expected maxima of the Mo atoms. These additional maxima were close to the ideal positions of the Cl atoms as derived from structure *A*. (The derivation was carried out in the same manner as described for the Mo atoms in §2.) Therefore they were taken as the real positions of the Cl atoms in structure *B*. They are shown schematically in Fig. 6(*a*) together with the real positions of the Mo atoms. The corresponding ideal positions calculated from the Mo and Cl maxima of the Fourier synthesis as well as those from the Mo and Cl positions of structure *A* are given in Fig. 6(*a*) and (*b*) by the ends of the arrows pointing to the atoms. The ideal positions of the Cl atoms in Fig. 6(*a*) and (*b*) do not coincide. It can be seen that the ideal positions for both Mo and Cl atoms are $z=0{\cdot}25$ in Fig. 6(*a*), while the corresponding ideal positions in Fig. 6(*b*) are Mo: $z=0{\cdot}25$ and Cl: $z<0{\cdot}25$.

The symmetry of the superstructure reflexions follows *mmm*. The usual integral extinctions are not observable. Therefore the structure causing the superstructure reflexions must be a primitive orthorhombic structure, provided that the reflexion symmetry is not generated by the superposition of reciprocal lattices of twins with lower symmetry than orthorhombic. However this possibility was rejected from the refinement of structure *B*.

Inspection of the Mo atoms in Fig. 6(*a*) leads to the following space-group symmetry elements: Mo(1) and Mo(2) are transformed into Mo(3) and Mo(4) respectively, by a *b* glide plane perpendicular to the *c* axis. The same is true for Mo(5) to Mo(8). These *b* glide planes cut the *c* axis at $z=0{\cdot}25$ and 0·75. Mo(1) to Mo(4) are transformed into Mo(5), Mo(8), Mo(7) and Mo(6) respectively, by *n* glide planes perpendicular to the *b* axis. The *n* glide planes cut the *b* axis at $y=0{\cdot}125$ and $y=0{\cdot}625$. As already mentioned above, the *a* axis is cut by mirror planes at $x=0$ and $x=0{\cdot}5$. These considerations are also true for the Cl atoms. The space group thus derived is therefore *Pmnb* [standard notation *Pnma*, the transformations into the usual description according to *International Tables for X-ray Crystallography* (1952) are given in the Appendix.] It must be noted, however, that the Fourier synthesis must show symmetry *Pmnb* because the model of the Mo atoms used for the phase calculation had this symmetry. It follows, that the Fourier map must show

Table 2. *The four models for structure-factor calculations*

	Model					Model			
Mo atoms	1	2	3	4	Mo atoms	1	2	3	4
Mo(1)	$+\Delta z$	$+\Delta z$	$+\Delta z$	$+\Delta z$	Mo(5)	$+\Delta z$	$-\Delta z$	$-\Delta z$	$+\Delta z$
Mo(2)	$+\Delta z$	$+\Delta z$	$+\Delta z$	$+\Delta z$	Mo(6)	$+\Delta z$	$+\Delta z$	$-\Delta z$	$-\Delta z$
Mo(3)	$-\Delta z$	$-\Delta z$	$-\Delta z$	$-\Delta z$	Mo(7)	$-\Delta z$	$+\Delta z$	$+\Delta z$	$-\Delta z$
Mo(4)	$-\Delta z$	$-\Delta z$	$-\Delta z$	$-\Delta z$	Mo(8)	$-\Delta z$	$-\Delta z$	$+\Delta z$	$+\Delta z$
					$R=\sum\|F_o-F_c\|/\sum F_o$	0·33	0·50	0·33	0·16

the *b* glide plane and that the ideal positions of Mo and Cl must necessarily have $z=0{\cdot}25$. As shown in Fig. 6(*b*) the *b* glide plane is not present if the ideal Mo and Cl positions have different *z* values. In this case the *b* glide plane has to be replaced by a 2_1 axis which leads to space group $Pmn2_1$.

7. Refinement of structure type *B*

To avoid refinement with a possibly wrong symmetry, the refinement was started in space group $Pmn2_1$ with the model shown in Fig. 6(*b*). The real positions used for the calculations are shown by the symbols of the atoms, the corresponding ideal positions by the end of the arrows.*

During the attempt at a refinement of the Mo and Cl positions in space group $Pmn2_1$ covariances up to |0·9| between corresponding parameters of the same kind of atoms were observed. The covariances were nearly removed by refining these parameters in subsequent least-squares cycles. The final *R* value was 0·12. From the refined real positions the ideal positions were recalculated. The displacements Δz of the real positions from the ideal positions were about 0·04 for Mo and 0·03 for Cl. The following *z* values of the ideal positions were obtained: $z(\mathrm{Mo})=0{\cdot}25$, $z(\mathrm{Cl})=0{\cdot}24$. A comparison with the starting *z* values shows that differences $z(\mathrm{Mo})-z(\mathrm{Cl})$ decreased during refinement. Furthermore the displacements Δ_z are larger than $z(\mathrm{Mo})-z(\mathrm{Cl})$. This also points towards the symmetry of the refined structure being very close to *Pmnb*.

In a second refinement the model shown in Fig. 6(*a*) was used. During refinement covariances larger than 0·6 were not observed. The *R* value dropped to 0·096. Because of this result the symmetry *Pmnb* was used for all further calculations.

As described above, in space group *Pmnb* all atoms of one kind form only one pseudo-equipoint. Each pseudo-equipoint is formed by two equipoints of space group *Pmnb*. Atoms of such two equipoints are connected by the relation derived from the pseudo-extinction rule. Atoms belonging to different equipoints are

* At this stage of the investigation it was assumed that the structure *A* is the average of the superstructure under investigation. Therefore the model of Fig. 6(*b*) was derived from structure *A*: a comparison of Figs. 1(*a*) and 6(*b*) shows that the positions of gravity derived from Fig. 6(*b*) for the Mo and Cl atoms are exactly the positions of these atoms in structure *A*.

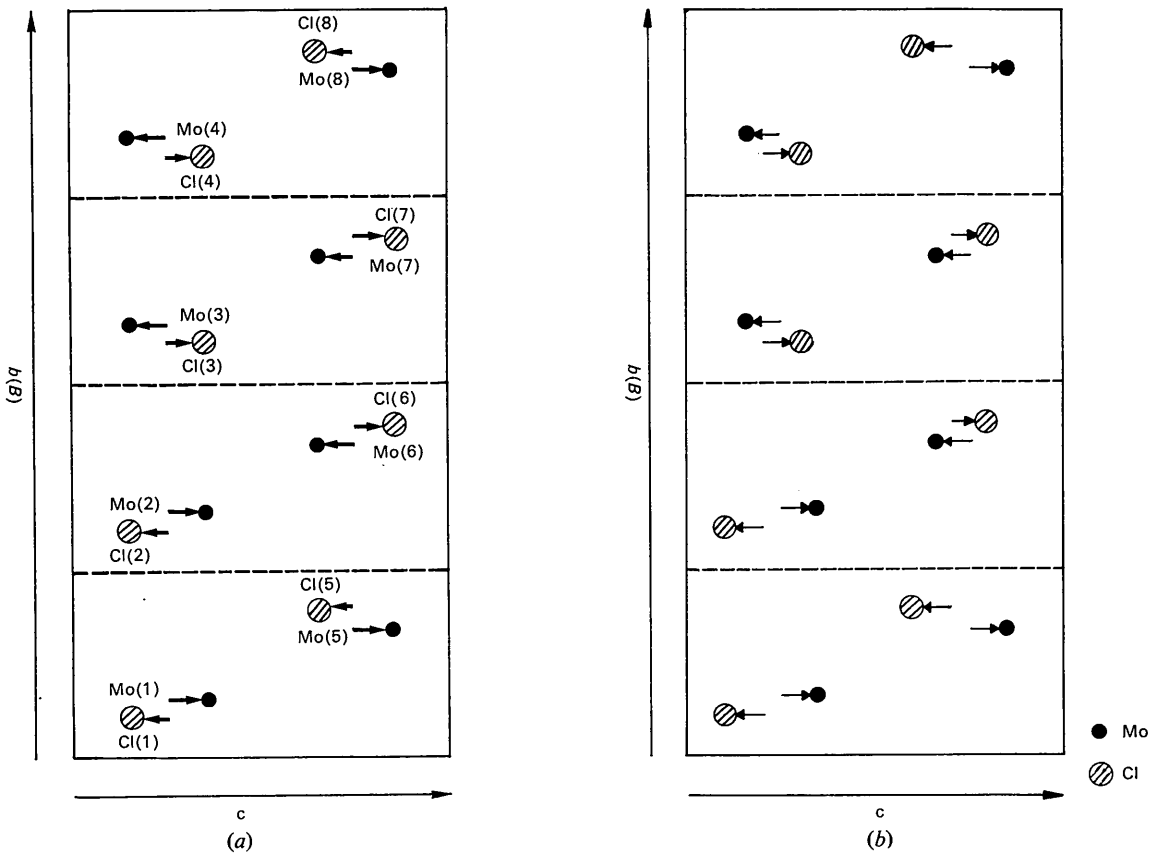

Fig. 6. (*a*) Superstructure model of Mo (small full circles) and Cl atoms taken from a Fourier synthesis with superstructure reflexions only. (*b*) Positions of Mo and Cl atoms in cell *B* derived from structure *A*. In (*a*) and (*b*) atoms are labelled as indicated or as in Fig. 3. The designation of the Cl atoms refers to two atoms related by a mirror plane perpendicular to the *a* axis. Shifts of atoms are highly exaggerated for clarity. All ideal positions are given by the ends of the arrows.

labelled in the following by I and by II [for example the atoms Mo(1), Mo(3), Mo(5) and Mo(7) of Fig. 6(*b*) form one equipoint and are designated as Mo(I)]. The coordinates of a general equipoint are given in Table 3. Cl atoms occupy twice the general equipoint, Mo atoms occupy twice equipoint 4(*c*). A Fourier synthesis showed that the atomic maxima of Mo(I) and Mo(II) as well as of Cl(I) and Cl(II) did not have equal heights. Therefore in a further calculation Mo(I), Mo(II), Cl(I) and Cl(II) were refined as independent equipoints. Covariances between z values and temperature factors were about |0·8|. All other covariances were smaller than |0·6|. The R value dropped to 0·079.

Table 3. *Coordinates of equivalent positions of structure B in space group Pmbn*

These are shown in Fig. 1(*b*)

x	y	z	
x	$0{\cdot}5+y$	$0{\cdot}5-z$	
$-x$	y	z	I
$-x$	$0{\cdot}5+y$	$0{\cdot}5-z$	
$0{\cdot}5+x$	$0{\cdot}25-y$	$0{\cdot}5+z$	
$0{\cdot}5+x$	$0{\cdot}75-y$	$-z$	
$0{\cdot}5-x$	$0{\cdot}25-y$	$0{\cdot}5+z$	II
$0{\cdot}5-x$	$0{\cdot}75-y$	$-z$	

With this structure model a difference-Fourier synthesis was calculated in order to find the oxygen atoms. Positions which could be related to O(3) of structure *A* were clearly resolved. These 8 oxygen positions again form two equipoints. These were also included in the refinement. From further difference-Fourier syntheses weak maxima were obtained near the ideal O(1) and O(2) positions (from structure *A*). These oxygens, forming four equipoints, were included in the refinement. The R value dropped to 0·061. During refinement corresponding O(1) and O(2) parameters showed covariances in the range of |0·9|. Therefore the coordinates of O(1) and O(2) must be applied rather carefully. Their errors are larger than given by the standard deviations.

During the final calculations the pseudo-extinct reflexions with $k=4n+2$ were included in the data set with $F_{obs}=0$. Anisotropic temperature factors were also applied. The R values at the end of the refinements are:

(*a*) With isotropic temperature factors,
- $R=0{\cdot}061$ for the observed superstructure reflexions only
- $R=0{\cdot}079$ for the observed superstructure reflexions plus the pseudo-extinct reflexions.

(*b*) With anisotropic temperature factors,
- $R=0{\cdot}059$ for the observed superstructure reflexions only
- $R=0{\cdot}074$ for the observed superstructure reflexions plus the pseudo-extinct reflexions.

The observed and calculated structure factors together with thoses of the pseudo-extinct reflexions are given in Table 4.

Table 4. *Structure factors and intensities*

(*a*) Superstructure reflexions with $F_o \neq 0$ ($k=2n+1$, $n=0, \pm 1, \pm 2, \ldots$).

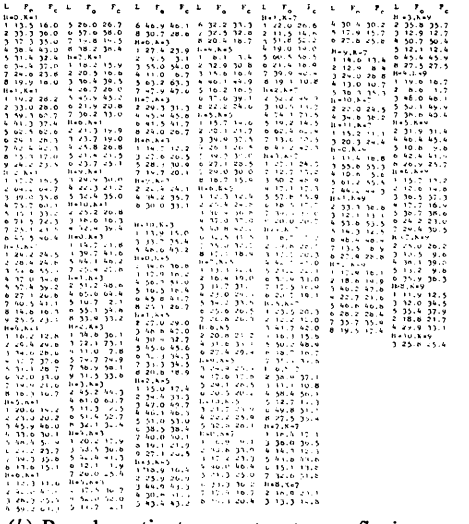

(*b*) Pseudo-extinct superstructure reflexions ($k=4n+2$, $n=0, \pm 1, \pm 2, \ldots$).

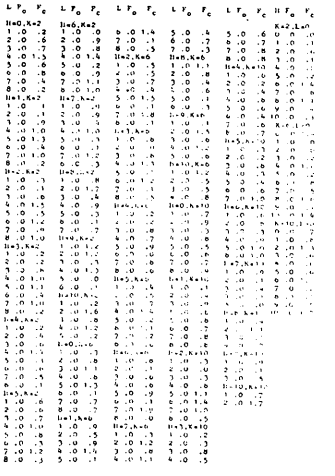

(*c*) Observed and calculated intensities of the main reflexions ($k=4n$, $n=0, \pm 1, \pm 2, \ldots$).
The intensities I_c were calculated by the formula:
$I_c = 0{\cdot}9F_A^2 + 0{\cdot}1F_B^2$.

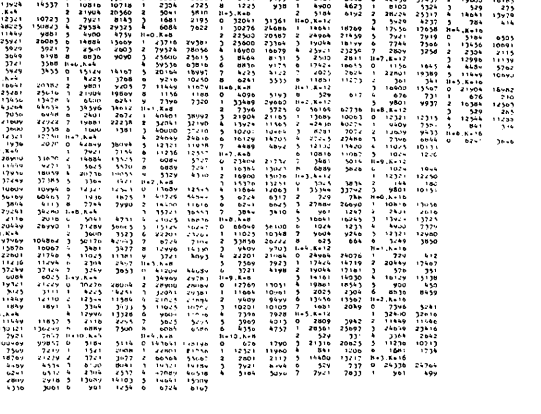

A comparison between the smallest observed and the largest calculated pseudo-extinct reflexion might be of interest. From Table 4 can be seen that $F_o(071)=6{\cdot}9$ and $F_c(10,10,2)=1{\cdot}7$. If one takes $[F_c(10,10,2)/F_o(071)]^2 = 0{\cdot}25^2 = 0{\cdot}06$. This result means that the largest pseudo-extinct reflexion has an intensity which is about 16 times smaller than the smallest observed intensity. Therefore all pseudo-extinct reflexions in the region of observation should have an intensity almost equal to zero, which is in agreement with the experimental results.

The structure parameters, bond distances and angles, main axes and orientation of thermal vibrational ellipsoids in the final model are listed in Tables 5, 6 and 7 respectively. The H_2O positions were identified from the Mo–O distances. Atoms labelled by (I) and (II) in Table 3 are related to each other by:

$$x(\mathrm{II}) \simeq x(\mathrm{I})$$
$$y(\mathrm{II}) \simeq y(\mathrm{I}) + \tfrac{1}{4}$$
$$z(\mathrm{II}) \simeq z(\mathrm{I}) .$$

A sign of equality would replace the sign of approximate equality in the above relations, if the pseudo-extinction rules holds exactly.

Table 5. *Atomic coordinates and temperature factors*

The atomic numbering scheme adopted is different from the intermediate one of Fig. 3. Labels 01, 02 and 03 respectively refer to the corresponding atoms in Schröder & Nørlund Christensen (1972).

Figures in parentheses are the standard deviations related to the last digit. Atoms labelled by (I) and (II) have the following relations:

$$x(\mathrm{II}) \simeq x(\mathrm{I}),\ y(\mathrm{II}) \simeq y(\mathrm{I}) + \tfrac{1}{4},\ z(\mathrm{II}) \simeq z(\mathrm{I}).$$

The anisotropic temperature factor was calculated in the form $\exp\ [-(\beta_{11}h^2+\beta_{22}k^2+\beta_{33}l^2+2\beta_{12}hk+2\beta_{13}hl+2\beta_{23}kl)]$.

	x	y	z	B [Å^2]
Mo(I)	0·0	0·0793 (2)	0·2928 (3)	0·82 (5)
Mo(II)	0·0	0·3296 (2)	0·2937 (5)	0·84 (5)
Cl(I)	0·2481 (7)	0·0568 (6)	0·2296 (4)	2·0 (1)
Cl(II)	0·2481 (8)	0·3066 (6)	0·2383 (5)	2·5 (2)
O1(I)	0·0	0·071 (3)	0·967 (5)	1·2 (10)
O1(II)	0·0	0·314 (3)	0·973 (5)	1·4 (10)
O2(I)	0·0	0·064 (3)	0·522 (5)	1·2 (10)
O2(II)	0·0	0·321 (3)	0·529 (5)	1·1 (10)
O3(I)	0·0	0·195 (3)	0·273 (2)	2·5 (7)
O3(II)	0·0	0·445 (4)	0·258 (2)	3·4 (10)

8. Generation of the diffraction pattern of a polycrystal containing volume elements of structures *A* and *B*

In Fig. 1(*b*) the structure is projected on (100). Structure *B* is subdivided into 4 'structure-*A*-sized' cells (separated from each other by broken lines).

In Fig. 1(*c*) these 4 '*A*-sized' cells are superimposed. This shows the so-called superposition or average structure of structure *B*. There, all atoms form so-called split atoms, for example the superimposed atoms Mo(1) to Mo(4) (*cf.* §2). By averaging the coordinates of the split positions the so-called positions of gravity are calculated. Furthermore water molecules and oxygen atoms are superimposed in one equipoint of average structure type *B*.

The symmetry of the superposition structure is *Pmnm*. Its symmetry and positions of gravity do not agree with the symmetry and atomic positions of structure *A*. This means that structure *A* is not the average structure of *B*, but that structures *A* and *B* exist in different parts of the investigated crystal grain. This crystal grain must therefore be considered as a polycrystal. The ratio of the volumes of these two structures can be approximately calculated from the scale factors of both structures. It is 2·5:1 after relating both factors to the large cell. It follows for the volumes that $V(A)/V(B)=(2{\cdot}5:1)^2$. This corresponds to about 85 volume % of structure *A* and about 15 volume % of structure *B* in the measured crystal grain. It follows that the influence of structure *B* on the structure investigation with the main reflexions can be nearly neglected. Only by interpretation of the weak superstructure reflexions is a determination of structure *B* possible.

Of course structure *B* must also produce reflexions with $k=4n$. This means that it also contributes to the so-called main reflexions. Thus the investigated crystal has to be regarded as being a crystal grain, containing volume parts of structures *A* and *B*. In order to check this result further, the main reflexions have been taken into account in the following way.

Structures *A* and *B* were used to calculate the *F* values of the main reflexions (reflexions with $k=4n$) with isotropic temperature factors. These two sets of *F* values are designated as $F_c(A)$ and $F_c(B)$. The reliability factors of F_o to $F_c(A)$ and $F_c(B)$ are 0·052 and 0·350 respectively.

Table 5 (*cont.*)

Coefficients of the anisotropic temperature factors

	β_{11}	β_{22}	β_{33}	β_{12}	β_{13}	β_{23}
Mo(I)	0·0026 (2)	0·0010 (2)	0·0038 (2)	0·0	0·0	0·0001 (2)
Mo(II)	0·0022 (2)	0·0010 (3)	0·0046 (3)	0·0	0·0	0·0002 (2)
Cl(I)	0·0045 (7)	0·0028 (7)	0·0101 (7)	0·0001 (5)	0·0000 (3)	−0·0002 (3)
Cl(II)	0·0042 (8)	0·0029 (7)	0·016 (1)	0·0001 (5)	0·0001 (4)	0·0005 (3)
O1(I)	0·004 (4)	0·000 (3)	0·006 (2)	0·0	0·0	0·001 (2)
O1(II)	0·005 (5)	0·000 (3)	0·008 (3)	0·0	0·0	0·002 (3)
O2(I)	0·001 (4)	0·002 (3)	0·006 (3)	0·0	0·0	−0·001 (3)
O2(II)	0·001 (4)	0·002 (3)	0·006 (3)	0·0	0·0	0·001 (2)
O3(I)	0·002 (3)	0·004 (5)	0·013 (4)	0·0	0·0	−0·001 (1)
O3(II)	0·002 (3)	0·005 (5)	0·024 (6)	0·0	0·0	0·0 (2)

Using the model of a polycrystal, the intensities of the main reflexions are generated by superposition of $I(A)=F_c^2(A)$ and $I(B)=F_c^2(B)$ according to their volume part in the investigated polycrystal. The calculated intensity

$$I_c=KF_c^2(A)+(1-K)F_c^2(B)$$

with K ranging from 0 to 1. K corresponds to the volume portion of structure A. A reliability factor of the intensities can now be calculated by

$$I_o=F_o^2$$
$$\Delta I=|s\,.\,I_c-I_o| \ (s\text{: scaling factor})$$
$$R=\sum\Delta I/\sum I_o\,.$$

This R value has been calculated in steps of $K=0{\cdot}05$. In Fig. 7 the plot of $R(I)$ against K is given. It shows a minimum at $K=0{\cdot}9$, corresponding to a 90 volume % of structure A and a 10 volume % of structure B in the investigated crystal grain. With the estimation that R related to F values is approximately one half of the R related to the intensities this minimum corresponds to a conventional $R=0{\cdot}039$. The obtained I_c values together with the F_o^2 values are listed in Table 4(*c*). This result is a further support for the model of a polycrystal. It is in good agreement with the volume ratio calculated from scale factors of both structures. Further proof of the model of the polycrystal would be possible with the aid of electron microscopy using superstructure reflexions for dark-field images. Unfortunately, the crystals of $MoO_2Cl_2 . H_2O$ are extremely moisture sensitive and sublime easily. Another possibility would be the refinement of structures A and B by a least-squares program for twins, which was not available to us.

9. Structure description

The basic element of the structures A and B is the coordination polyhedron of Mo in the form of a distorted octahedron which is shown *e.g.* in Fig. 2.

Table 6. *Interatomic distances and angles*

These should be compared with Fig. 1(*b*).

Numbers given in parentheses are the standard deviations related to the last digit. Atoms labelled ''' are those in the neighbouring cell in the *c* direction. Also included are O1(I') and O1(II'). Atoms Mo(II'), O1(II'') and O3(II') are taken into the cell shown although they belong to the neighbouring cell in the -*b* direction.

Mo(I) octahedron			
Mo(I)–O2(I)	1·60 (3) Å	Cl(I)–Mo(I)–Cl(I)	152·5 (3)°
Mo(I)–O3(II')	2·12 (6)	Cl(I)–Mo(I)–O1(I') (H_2O)	78·8 (2)
Mo(I)–O1(I') (H_2O)	2·25 (3)	Cl(I)–Mo(I)–O2(I)	99·3 (3)
Mo(I)–O3(I)	1·81 (5)	Cl(I)–Mo(I)–O3(I)	97·6 (3)
Mo(I)–Cl(I)	2·357 (7)	Cl(I)–Mo(I)–O3(II')	79·8 (2)
Cl(I)–O1(I') (H_2O)	2·93 (2)	O1(I') (H_2O)–Mo(I)–O2(I)	168 (2)
Cl(I)–O2(I)	3·06 (2)	O1(I') (H_2O)–Mo(I)–O3(I)	89 (1)
Cl(I)–O3(I)	3·16 (3)	O1(I') (H_2O)–Mo(I)–O3(II')	77 (1)
Cl(I)–O3(II')	2·88 (4)		
Cl(I)–O1(I'') (H_2O)	3·47 (3)	O2(I)–Mo(I)–O3(I)	103 (2)
		O2(I)–Mo(I)–O3(II')	91 (2)
O1(I) (H_2O)–O2(I)	3·08 (5)	O3(I)–Mo(I)–O3(II')	166·1 (7)
O1(I') (H_2O)–O3(I)	2·87 (5)		
O1(I') (H_2O)–O3(II')	2·72 (5)	Cl(I)—O1(I') (H_2O)–Cl(I)	103 (1)
		O3(I)—O1(I') (H_2O)–O3(II')	88 (2)
O2(I)–O3(I)	2·67 (6)	O3(I)—O1(I') (H_2O)–O2(I''')	139 (2)
O2(I)–O3(II')	2·68 (6)	O3(II')–O1(I') (H_2O)–O2(I''')	132 (2)
Mo(II) octahedron			
Mo(II)–O3(I)	2·09 (5) Å	Cl(II)–Mo(II)–Cl(II)	154·2 (4)°
Mo(II)–O2(II)	1·63 (3)	Cl(II)–Mo(II)–O1(II') (H_2O)	79·7 (2)
Mo(II)–O3(II)	1·82 (6)	Cl(II)–Mo(II)–O2(II)	98·7 (3)
Mo(II)–O1(II') (H_2O)	2·23 (3)	Cl(II)–Mo(II)–O3(I)	80·6 (2)
Mo(II)–Cl(II)	2·349 (7)	Cl(II)–Mo(II)–O3(II)	97·4 (3)
Cl(II)–O1(II') (H_2O)	2·94 (2)	O1(II') (H_2O)–Mo(II)–O2(II)	169 (2)
Cl(II)–O2(II)	3·06 (2)	O1(II') (H_2O)–Mo(II)–O3(I)	80 (1)
Cl(II)–O3(I)	2·88 (3)	O1(II') (H_2O)–Mo(II)–O3(II)	88 (1)
Cl(II)–O3(II)	3·15 (4)		
Cl(II)–O1(II'') (H_2O)	3·33 (3)	O2(II)–Mo(II)–O3(I)	90 (2)
		O2(II)–Mo(II)–O3(II)	102 (2)
O1(II) (H_2O)–O2(II)	3·07 (5)		
O1(II') (H_2O)–O3(I)	2·78 (5)	O3(I)–Mo(II)–O3(II)	168·1 (7)
O1(II') (H_2O)–O3(II)	2·83 (6)		
O2(II)–O3(I)	2·64 (6)	Cl(II)—O1(II') (H_2O)–Cl(II)	102 (1)
O2(II)–O3(II)	2·69 (6)	O3(I)—O1(II') (H_2O)–O3(II)	88 (2)
		O2(II''')–O1(II') (H_2O)–O3(I)	140 (2)
		O2(II''')–O1(II') (H_2O)–O3(II)	132 (2)
		Mo(I)–O3(I)—Mo(II)	171·6 (8)
		Mo(I)–O3(II')–Mo(II')	178·3 (9)

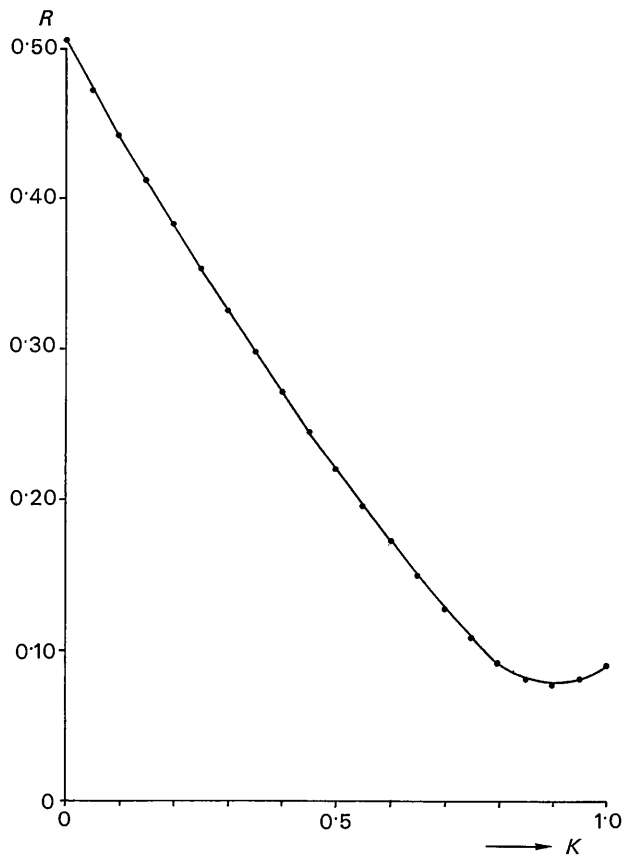

Fig. 7. Plot of $R=\sum\Delta I/\sum I_o$ of the investigated polycrystal for different ratios $V(A):V(B)$.

The Mo atom is displaced from the centre into a tetrahedral environment shown by the heavy lines. The linkage of these polyhedra is different in structures *A* and *B*.

Fig. 2 shows the chains of polyhedra in structure *A* through two unit cells. In Fig. 8 these cells are inverted so that **c** is changed into $-\mathbf{c}$. This arrangement is designated as structure $\bar{A}$. Both arrangements can be determined with the same data set because of the intensity relation $I(hkl)=I(hk\bar{l})$. Fig. 9 shows structure *B*. It is built of chains of octahedra too. The chains are again antiparallel. The non-periodic part of a chain contains 4 octahedra. A comparison with Figs. 2 and 8 proves that each chain contains two octahedra of structure *A* and two of $\bar{A}$. The unit cell in Fig. 9 is subdivided into 4 'structure-*A*-sized' cells, which should be numbered 1 to 4 in the direction of increasing *y* value. A comparison of Fig. 2 with Fig. 9 shows that the unit cell of structure *A* agrees with subcell 1 and the unit cell of structure $\bar{A}$ agrees with subcell 3. The remaining subcells 2 and 4 contain octahedra of both structures *A* and $\bar{A}$.

Thus, structures *A* and *B* have to be considered as polytypes: two different structures are built up with

Table 7. *Main axes and orientation of the thermal vibrational ellipsoids*

	Mo(I)				Mo(II)				O1(I)				O1(II)			
Length of main axes [Å]	0·095 (3)	0·105 (4)	0·11 (1)	0·097 (5)	0·102 (8)	0·11 (1)	0·04 (36)		0·13 (5)	0·14 (6)	0·03 (47)		0·14 (8)	0·16 (5)		
Angle with *a* axes [°]	90	0	90	0	90	90	90		90	0	90		0	90		
Angle with *b* axes [°]	81 (17)	90	171 (17)	90	55 (44)	145 (44)	154 (64)		64 (64)	90	154 (42)		90	116 (42)		
Angle with *c* axes [°]	171 (17)	90	99 (17)	90	145 (44)	125 (44)	64 (64)		26 (64)	90	64 (42)		90	154 (42)		
		Cl(I)			Cl(II)				O2(I)				O2(II)			
	0·14 (1)	0·156 (6)	0·18 (2)	0·13 (1)	0·18 (2)	0·202 (8)	0·1 (1)		0·12 (3)	0·2 (1)	0·1 (1)		0·12 (5)	0·2 (1)		
	1 (15)	90 (12)	89 (14)	2 (11)	91 (12)	88 (5)	0		90	90	0		90	90		
	89 (15)	84 (11)	174 (11)	88 (12)	28 (32)	118 (32)	90		78 (56)	168 (56)	90		64 (92)	154 (92)		
	90 (11)	6 (11)	84 (11)	89 (4)	118 (32)	152 (32)	90		12 (56)	78 (56)	90		154 (92)	116 (92)		
									O3(I)				O3(II)			
									0·18 (3)	0·2 (1)	0·09 (7)		0·23 (7)	0·24 (7)		
									90	90	0		90	90		
									79 (38)	169 (38)	90		43 (180)	133 (180)		
									11 (38)	79 (38)	90		133 (180)	137 (180)		

the same main structure element, the coordination polyhedron around the Mo atoms. As a consequence it has to be assumed that the crystal contains volume elements of the structures *A*, $\bar{A}$ and *B* as shown schematically in Fig. 10.

Structures *A*, $\bar{A}$, *B* are characterized by octahedra chains parallel to the *b* axis. It is obvious that each octahedron also acts as a dipole, the direction of which is parallel to the *c* axis. A comparison of Figs. 2,8 and 9 shows that these dipoles are parallel in structures *A* and $\bar{A}$, but that in structure *B* they are partly parallel and partly antiparallel. It is likely that this difference in dipole orientation explains the different volume ratios of structures *A* and $\bar{A}$ on the one hand and structure *B* on the other.

A comparison of the bond distances and angles of Table 6 between the two independent coordination polyhedra shows good agreement between the corresponding values. The comparison with those of structure *A* exhibits no serious differences, as would be expected from the foregoing discussion. The greatest differences – as might have been expected – occur at the bridging Mo–O bonds, where the (short) distances within the coordination polyhedra are extended to 1·81 (5) and 1·82 (6) Å in comparison with 1·678 (14) Å in structure *A*. In addition the terminal Mo–O distances are shortened somewhat to 1·60 (3) and 1·63 (3) Å in comparison with 1·671 (10) Å in structure *A*. Although the resulting differences may not be significant, they appear to be reasonable, as it can be expected that the differences between terminal and bridging Mo–O distances should be somewhat greater than between 1·671 and 1·678 Å.

F. S. thanks the Deutsche Forschungsgemeinschaft for financial support. The calculations were done on CDC 6400/6500 and IBM 7040 computers. We are indebted to the Carlsberg Fonden for the use of the diffractometer in Aarhus, were the intensities were collected.

APPENDIX

In the following, a general formulation for the general equipoint of space group *Pmnb* is given. Because the choice of the origin of the unit cell is as described, it holds that

the mirror plane *m* cuts the *a* axis at $x=p$,
the glide plane *n* cuts the *b* axis at $y=q$,
the glide plane *b* cuts the *c* axis at $z=r$.

According to this the equivalent positions of the general equipoint have the following coordinates:

1.		x,		y,		z
2.		x,	0·5+	y,	$2r-$	z
3.	$2p-$	x,		y,		z
4.	$2p-$	x,	0·5+	y,	$2r-$	z
5.	0·5+	x,	$2q-$	y,	0·5+	z
6.	0·5+	x,	$0{\cdot}5+2q-y$,		$-0{\cdot}5+2r-z$	
7.	$-0{\cdot}5+2p-x$,		$2q-$	y,	0·5+	z
8.	$-0{\cdot}5+2p-x$,		$0{\cdot}5+2q-y$,		$-0{\cdot}5+2r-z$	

For the origin chosen in this paper *p*, *q*, *r* have the following values (*cf.* Table 3): $p=0$; $q=\frac{1}{8}$; $r=\frac{1}{4}$. In the usual setting of *International Tables for X-ray Crys-*

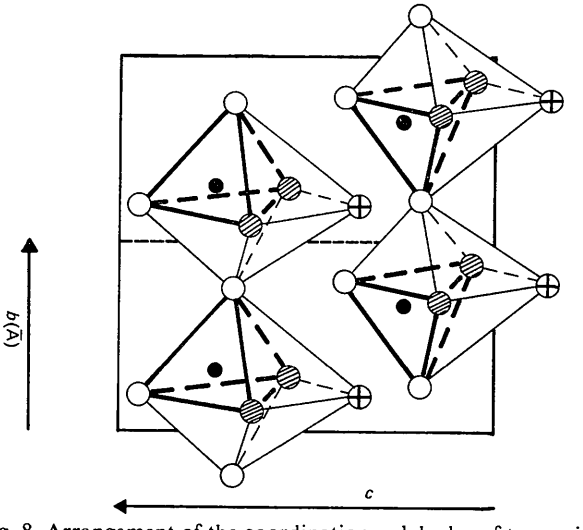

Fig. 8. Arrangement of the coordination polyhedra of two unit cells of structure $\bar{A}$.

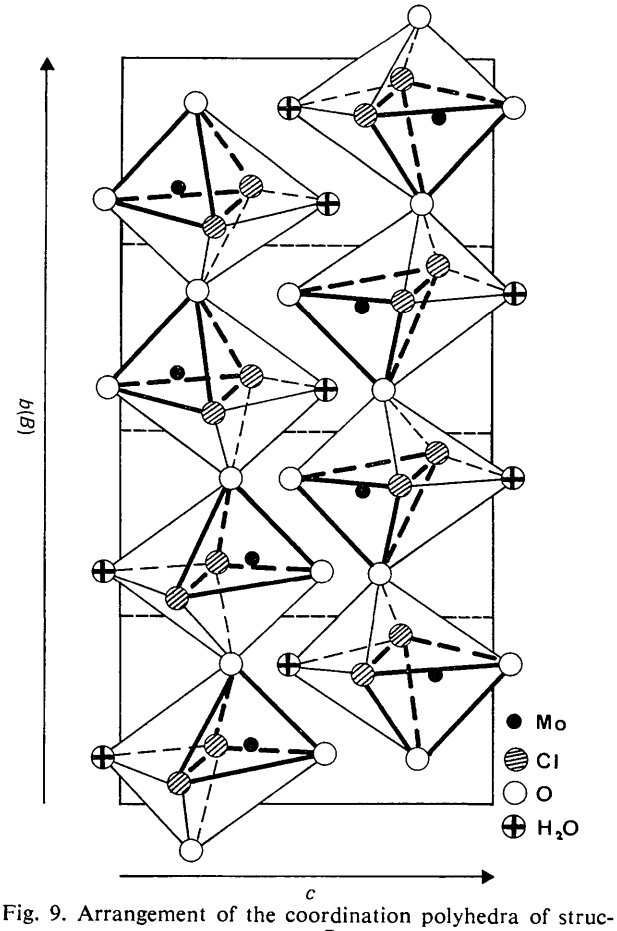

Fig. 9. Arrangement of the coordination polyhedra of structure *B*.

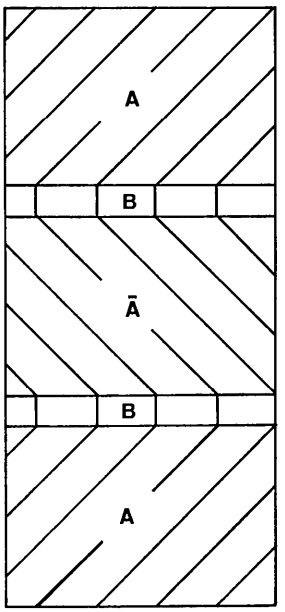

Fig. 10. Schematic presentation of the domain regions of structures A, $\bar{A}$ and B respectively in the investigated crystal grain.

tallography (1952), for space group *Pmnb* the relationship $p=\frac{1}{4}$, $q=\frac{1}{4}$, $r=\frac{1}{4}$ exists. Therefore, the transformation of the coordinates of the setting of this paper (designated as x,y,z) into that of the usual setting (designated as x',y',z') is given by

$$x'=x+\tfrac{1}{4}$$
$$y'=y+\tfrac{1}{8}$$
$$z'=z\,.$$

Pmnb can be transformed into the standard notation *Pnma* by $\mathbf{a}\rightarrow\mathbf{b}$, $\mathbf{b}\rightarrow\mathbf{a}$, $\mathbf{c}\rightarrow-\mathbf{c}$.

References

ATOVMYAN, L. O. & ALIEV, Z. G. (1971). *Zh. strukt. Khim.* **12**, 732–734

BUSING, W. R., MARTIN, K. O. & LEVY, H. A. (1962). *ORFLS*. Report ORNL-TM305, Oak Ridge. National Laboratory, Oak Ridge, Tennessee.

International Tables for X-ray Crystallography (1952). Vol. I. Birmingham: Kynoch Press.

NIGGLI, A. (1959). *Z. Kristallogr.* **111**, 283–287.

SCHRÖDER, F. A. & NØRLUND CHRISTENSEN, A. (1972). *Z. anorg. allgem. Chem.* **392**, 107–123.

Acta Cryst. (1973). A**29**, 333

Polycrystals and Stereochemistry of $MoO_2Cl_2.H_2O$*

BY F. A. SCHRÖDER

Lehrstuhl für Anorganische Chemie der Universität, D – 7800 Freiburg i. Br., Albertstrasse 21, Germany (BRD)

AND H. SCHULZ

Institut für Kristallographie und Petrographie, ETH, CH – 8006 Zürich, Sonneggstrasse 5, Switzerland

(*Received* 23 *April* 1972; *accepted* 8 *February* 1973)

Based on the results of the preceding paper by H. Schulz & F. A. Schröder [*Acta Cryst.* (1973), A**29**, 322–333] the diffuse diffraction pattern of crystals of $MoO_2Cl_2.H_2O$ as observed by L. O. Atovmyan & Z. G. Aliev [*Zh. Strukt. Khim.* (1971), **12**, 732–734] is explained. Furthermore the types of polycrystals which can be expected to exist are deduced. This leads to a detailed understanding of the stereochemistry of this compound. Several aspects of the crystal growth are discussed.

Introduction

A characteristic of the stereochemistry of molybdenum and tungsten is structures built of endless chains of octahedra by sharing two *trans* vertices. Only compounds of these two elements in the oxidation state +VI form such structures using only monatomic ligands such as oxygen and halogen atoms at the vertices of electrostatically neutral octahedra.

According to the most recent results for the determination of the structure of $MoO_2Cl_2.H_2O$ by Atovmyan & Aliev (1971), Schröder & Nørlund Christensen (1972) and Schulz & Schröder (1973) this compound also forms such chains of octahedra. These have mixed ligands and the composition $MoCl_2OO^{2}/^{2}OH_2$. In the following some stereochemical aspects of these chains are discussed.

Results

In the preceding paper of Schulz & Schröder (1973) the results of a structural investigation of a polycrystal

* Part XII of Contributions to the Chemistry of Molybdenum and Tungsten. For part XI see: *Z. Naturforsch.* (1973), 46–55.